

# Myelin Transcription Factor 1 (Myt1) of the Oligodendrocyte Lineage, Along With a Closely Related CCHC Zinc Finger, Is Expressed in Developing Neurons in the Mammalian Central Nervous System

Jin G. Kim,<sup>1</sup> Regina C. Armstrong,<sup>2</sup> Denes v. Agoston,<sup>3</sup> Alexandra Robinsky,<sup>1</sup> Claudia Wiese,<sup>4</sup> James Nagle,<sup>5</sup> and Lynn D. Hudson<sup>1\*</sup>

<sup>1</sup>Laboratory of Developmental Neurogenetics, National Institute of Neurological Disorders and Stroke, National Institutes of Health, Bethesda, Maryland

<sup>2</sup>Department of Anatomy and Cell Biology, Uniformed Services University of the Health Sciences, Bethesda, Maryland

<sup>3</sup>Laboratory of Developmental Neurobiology, National Institute of Child Health and Human Development, National Institutes of Health, Bethesda, Maryland

<sup>4</sup>Preclinical Research, Hoffmann-La Roche, Basel, Switzerland

<sup>5</sup>Sequencing Facility, National Institute of Neurological Disorders and Stroke, National Institutes of Health, Bethesda, Maryland

The establishment and operation of the nervous system requires genetic regulation by a network of DNA-binding proteins, among which is the zinc finger superfamily of transcription factors. We have cloned and characterized a member of the unusual Cys-Cys-His-Cys (also referred to as Cys<sub>2</sub>HisCys, CCHC, or C2HC) class of zinc finger proteins in the developing nervous system. The novel gene, *Myt1*-like (*Myt1l*), is highly homologous to the original representative of this class, *Myelin transcription factor 1* (*Myt1*) (Kim and Hudson, 1992). The *MYT1* gene maps to human chromosome 20, while *MYT1L* maps to a region of human chromosome 2. Both zinc finger proteins are found in neurons at early stages of differentiation, with germinal zone cells displaying intense staining for *Myt1*. Unlike *Myt1*, *Myt1l* has not been detected in the glial lineage. Neurons that express *Myt1l* also express *TuJ1*, which marks neurons around the period of terminal mitosis. The *Myt1l* protein resides in distinct domains within the neuronal nucleus, analogous to the discrete pattern previously noted for *Myt1* (Armstrong et al.: 14:303–321, 1995). The developmental expression and localization of these two multifingered CCHC proteins suggests that each may play a role in the development of neurons and oligodendroglia in the mammalian central nervous system. *J. Neurosci. Res.* 50:272–290, 1997. © 1997 Wiley-Liss, Inc.†

**Key words:** zinc finger; transcription factor; differentiating neurons; oligodendrocyte progenitors; myelin

## INTRODUCTION

A burgeoning number of proteins have been found to contain domains that fold when stabilized by bound zinc ions (reviewed by Berg and Shi, 1996). These zinc finger proteins function in a variety of DNA–protein and protein–protein interactions and include a host of transcription factors that are found in the nervous system. The transcription factor TFIIIA is the prototype of the Cys<sub>2</sub>HisCys class of zinc finger proteins, one of the over ten different structural classes of zinc fingers which already has several thousand members. *Myt1* represents a novel structural class of zinc fingers, based on the Cys<sub>2</sub>HisCys (CCHC) coordination chemistry and secondary structure predictions (Kim and Hudson, 1992). In addition, based upon primary sequence comparisons, the *Myt1* class differs markedly from the other class of Cys<sub>2</sub>HisCys fingers, typified by the retroviral nucleocapsid proteins (Covey, 1986). Moreover, circular dichroism spectra studies suggest that a metal-bound *Myt1* zinc finger lacks

Abbreviations: *Myt1*, rodent myelin transcription factor 1; *MYT1*, human myelin transcription factor 1; *Myt1l*, rodent myelin transcription factor 1-like; *MYT1L*, human myelin transcription factor 1-like; PLP, proteolipid protein.

Contract grant sponsor: USUHS; Contract grant number: R070CB.

The first two authors contributed equally to this work.

\*Correspondence to: Lynn D. Hudson, National Institute of Neurological Disorders and Stroke, Building 36, Room 5D06, 36 Convent Dr MSC 4160, Bethesda, MD 20892-4160. E-mail: hudson@helix.nih.gov

Received 18 May 1997; Accepted 5 June 1997

the  $\alpha$ -helix and  $\beta$ -sheet secondary structure typical of Cys<sub>2</sub>His<sub>2</sub> fingers (E.H. Cox, M.C. Posewitz, and D.E. Wilcox, personal communication) and further support the structural uniqueness of Myt1.

Myt1 was originally cloned in a screen for DNA-binding proteins that recognize *cis* elements in the promoter region of the most abundantly expressed myelin protein, proteolipid protein (PLP) (Berndt et al., 1992; Kim and Hudson, 1992). Myt1 was found to be highly expressed in cells of the subventricular zone (Armstrong et al., 1995), a germinal area from which neurons, astrocytes, and oligodendrocytes arise, suggesting that this DNA-binding protein may influence the differentiation of neural progenitors. Moreover, Myt1 was present at the earliest stage of the oligodendrocyte lineage that could be identified in culture (i.e., cells that are immunopositive for nestin and polysialic acid N-CAM antibodies) and was maintained until oligodendrocytes matured (Armstrong et al., 1995). Recently, the isolation of the *Xenopus* form of Myt1 has established a role for Myt1 in neuronal differentiation in the invertebrate nervous system (Bellefroid et al., 1996). *Xenopus* Myt1 is capable of inducing neuronal differentiation when expressed ectopically, and mutations which interfere with Myt1 function inhibit normal neurogenesis (Bellefroid et al., 1996). While invertebrates appear to have only a single representative of the Myt1 class of Cys<sub>2</sub>HisCys zinc fingers in the nervous system, vertebrates possess at least two. (Wiese et al., 1995). We report here the cloning and characterization of a highly homologous family member of Myt1, designated Myt1-like (Myt1l) in mouse and MYT1-like (MYT1L) in man, together with the chromosomal localization of Myt1 and the Myt1l family member. Our results document the expression of both Myt1 and Myt1l protein and mRNA in immature neurons of the murine CNS. A comparison of the neuronal expression of Myt1l with the combined neuronal and glial expression of Myt1 suggests that these two zinc finger proteins play distinct roles in the developing nervous system.

## MATERIALS AND METHODS

### Cloning of Mouse Myt1 and Myt1l cDNAs

To obtain the mouse cDNA for Myt1, total RNA from mouse embryonic day 11 was reverse transcribed to produce single-stranded cDNA, and then Myt1-specific cDNAs were amplified by polymerase chain reaction (PCR) using primers from the 5' untranslated region and the coding region (amino acids 561–568) of a Myt1 genomic clone (CW009). The sense primer was 5'-GTTCTCAGACACCAAGAGCAGGTAC-3', and the antisense primer was 5'-ATTGGAAGGCTTTGGGTGAG-GTTTC-3'. Approximately 2 kb of the 3' untranslated

region was cloned by rapid amplification of cDNA ends using the cDNA Amplification kit (Clontech, Palo Alto, CA). The primers designed for this region and the coding region were used to produce PCR products. The sense primer was 5'-AAGAGCAGCTACAGTAGCTACCAGG-3', and the antisense primer was 5'-AACACACCAC-GAGGTACTGTGAGTC-3'. PCR was carried out for 30 cycles: at 94°C for 1 min, at 60°C for 2 min, and at 72°C, 3 min. The resulting PCR products were subcloned into the pCRII vector using a TA cloning kit (Invitrogen, San Diego, CA) and sequenced.

The original Myt1l cDNA was initially cloned as an expressed sequence tag from a human brain cDNA library (Adams et al., 1993). The original clone, HFBEE29 (corresponding to EST05024), was purchased from American Type Culture Collection (ATCC; Rockville, MD) and was used for further extended screening with a human fetal brain cDNA library (Stratagene, La Jolla, CA). In total, about  $1 \times 10^6$  plaques were screened. The positive clones were converted to plasmid by the *in vivo* excision procedure described by the manufacturer and sequenced using a sequenase 2.0 kit (U.S. Biochemical Corp., Cleveland, OH). To obtain the mouse cDNA clone for Myt1l, primers whose sequence was based on the human cDNA clone were used in a PCR amplification reaction, together with cDNA prepared from mouse total RNA. The sense primer was 5'-ATTTCTCGAGCAAGTGTC-CAACCC-3', and the antisense primer was 5'-TGTC-CAGACAGCAGCAGCTATAAAC-3'. 5' and 3' regions of the cDNA were isolated using the cDNA Amplification kit (Clontech, Palo Alto, CA) according to manufacturer's instructions.

### Chromosome Mapping

For mapping the human *MYT1* and *MYT1L* genes, a blot containing BamHI-digested genomic DNA from a panel of monochromosomal human/rodent hybrid cell lines (Oncor, Gaithersburg, MD) was probed with radiolabeled Myt1 or Myt1l cDNA. Both probes were generated by first amplifying a cDNA segment from the human MYT1 plasmid (pMYT1a) or the human MYT1L plasmid (pHEB4), and then random priming (Gibco/BRL, Gaithersburg, MD) the gel-purified 215-bp Myt1 product (amino acids 604–736) and the 398-bp Myt1l product (amino acids 497–568) with [<sup>32</sup>P]- $\alpha$ -dCTP. For the MYT1 probe, the PCR reaction included 3 ng of template and 500 ng of each primer (E1H; 5'-GCCCATGTGTTTTGT-GAAGCAGCTC-3', E2H; 5'-ATTGAAAGGCTTTAG-GTGAGGTTTC-3') and was cycled 30 times at 95°C for 1 min, then 60°C for 2 min and 72°C for 3 min. For the MYT1L probe, the PCR reaction included 10 ng of template and 500 ng of each primer (H10; 5'-GCTCAG-GCCAATGTGCTTTGTGAAG-3', H11; 5'-CTCCAT-

GTCGTGCGTGTAGTCGAAG-3') and was cycled 30 times at 94°C for 1 min, then 55°C for 2 min and 72°C for 3 min. Hybridization was carried out at 42°C for 16 hr in 50% formamide, 5× Denhardt's solution, 5× SSPE (0.75M NaCl, 50 mM NaH<sub>2</sub>PO<sub>4</sub>, 5mMEDTA), 1% sodium dodecyl sulfate (SDS), 100 µg/ml herring sperm DNA. Nonspecifically bound probe was removed by washing the membrane three times, 1 hr per wash, in 0.2× SSC with 1% SDS at 55°C. Under these conditions of hybridization stringency, the human MYT1 probe can bind to both the rodent and human Myt1 genomic fragments; likewise, the human MYT1L probe can bind both the rodent and human Myt1l fragments present on the blot.

### Northern Analysis

RNA was isolated from enriched populations of cultured O-2A progenitors, oligodendrocytes, or astrocytes (each prepared as described in Armstrong et al., 1995), as well as brain, spinal cord, and sciatic nerve from postnatal day 2 rat, according to the procedure of Chomczynski and Sacchi (1987). Poly A<sup>+</sup> RNAs from different stages of the rat development were prepared according to the manufacturer's protocol (Promega polyAtract kit). Total RNA (2 µg per lane) or poly A<sup>+</sup> RNA (1 µg per lane) was fractionated by electrophoresis through 1% formaldehyde/agarose gels, transferred to nitrocellulose, and hybridized with a digoxigenin-labeled riboprobe for Myt1 or Myt1l. Riboprobes were prepared which would hybridize with the 3' untranslated region of each gene to differentially detect Myt1 relative to the Myt1l. Each probe was transcribed *in vitro* and labeled with digoxigenin (DIG-11-UTP, Boehringer Mannheim, Indianapolis, IN). The 1.5-kb PstI fragment from rat Myt1 cDNA was cloned into the pGEM-3Z vector (Promega, Madison, WI). The resulting plasmid (pR-PST) was linearized with XbaI and transcribed with SP6 RNA polymerase to give a 1.5-kb riboprobe. The 0.7-kb BamHI fragment from rat Myt1l cDNA was cloned into pGEM-3Z. This plasmid (pR-BAM) was linearized with SmaI and transcribed with SP6 RNA polymerase to give a 700-base riboprobe. A PLP riboprobe was used as a positive control. PLP cDNA (from pLH 116) was linearized with EcoRI and transcribed with SP6 polymerase to give a 980-base riboprobe. Hybridization and detection steps were followed according to the manufacturer's instruction (Boehringer Mannheim).

Rat cyclophilin (Milner and Sutcliff, 1983) and human β-actin (Cleveland et al., 1980) probes were used as internal standards.

### In Situ Hybridization

Postnatal day 3 rats were perfused with 4% paraformaldehyde, and frozen sections of spinal cord were

prepared, as detailed in Armstrong et al. (1995). *In situ* hybridization was performed on tissue sections according to the procedure described for cultured cells (Armstrong et al., 1995), with the addition of a 15-min 37°C digestion with proteinase K (10 mg/ml) prior to acetylation and hybridization. Hybridizations with digoxigenin probes specific for the 3' untranslated region of the rat Myt1 or Myt1l, or for PLP (as described above for the Northern analysis), were performed in parallel during each experiment.

### Antibody Production and Immunoblot Analysis

An antiserum directed against a synthetic peptide corresponding to an internal region of Myt1l (amino acid residues 207–223 in Fig. 1) was produced in New Zealand white rabbits by Research Genetics (Huntsville, AL). The synthetic Myt1l peptide (LGKIAEDAAAYRARTESE) was not homologous to any region in the Myt1 protein. The anti-Myt1l peptide antibody titer was determined by enzyme-linked immunosorbent assay (ELISA) with the peptide on the solid phase. To affinity purify the antibody, first a Myt1l-His fusion protein containing the amino acid residues used in antiserum production (Nos. 207–223) was constructed: a PCR product with XhoI ends, extending from positions 1263–1842 of the nucleotide sequence in Figure 1, was cloned into the XhoI site of pET16b for expression of His-tagged Myt1l in bacteria. Then the recombinant protein was expressed essentially as in Armstrong et al. (1995). The anti-peptide antibody was purified on a nickel-NTA column, to which the Myt1l-His fusion protein was preabsorbed, and the antibody was subsequently eluted with 4 M MgCl<sub>2</sub> (Gu et al., 1994).

For immunoblot analysis, proteins were resolved on a 4–20% SDS-polyacrylamide gel electrophoresis (PAGE) gel and electrophoretically transferred to a nitrocellulose membrane, which was blocked by pretreating for 1 hr at room temperature in 5% nonfat dry milk in phosphate-buffered saline (PBS) containing 0.1% Tween 20 (TPBS). Primary antibody to Myt1 (αMyt1-His, from amino acids 541–727 of the Myt1 protein, described in Armstrong et al., 1995) was used at a 1:1,000 dilution, and antiserum to Myt1l was used at 1:750 dilution, each in TPBS with 0.5% nonfat dry milk. Antibodies were incubated with the membranes for 1 hr. After washing with TPBS, antigen-antibody complexes were visualized with horseradish peroxidase-conjugated donkey anti-rabbit secondary antibody (diluted 1:4,000 in TPBS) and enhanced chemiluminescence detection reagents (ECL kit; Amersham, Arlington Heights, IL), following the manufacturer's instructions.





### Culturing of Primary Embryonic Neurons

Embryonic neurons were isolated from E16 rat (Sprague-Dawley, Taconic Farms, MD) forebrains. Timed-pregnant mothers were sacrificed by cervical dislocation, embryos along with the uterine wall were collected on ice, and heads were collected into isotonic ice-cold D1 cell dissection medium (Agoston et al., 1991). Parietal cortex, striatal primordium, and the diencephalon were dissected from coronal slices and transferred into fresh ice-cold D1 medium. The collected brain regions were washed once with 15 ml prewarmed and equilibrated Hanks' balanced salt solution, and cells were dissociated using the papain cell dissociation system according to the manufacturer's instructions (Worthington). Cells were plated into poly-L-lysine-precoated 8-well chamber slides at a density of 25,000 cells per well and maintained at 37°C in 10% CO<sub>2</sub>. The plating medium was MEM (GIBCO BRL) containing N3 nutrient mixture (Agoston et al., 1991), 2 mM glutamine, antibiotic-antimycotic mixture (GIBCO BRL), 10% heat-inactivated bovine serum, and 10 µg/ml platelet-derived growth factor (PDGF; Peprotech, Rocky Hill, NJ). After 8–12 hr of plating, the medium was changed to maintaining medium: minimum essential medium (MEM) containing N3 nutrient mixture, 2 mM glutamine, antibiotic-antimycotic mixture, 1% heat-inactivated fetal calf serum, 10 µg/ml PDGF, and 0.3 mg/ml bovine serum albumin (BSA; Sigma, St. Louis, MO). Half of the medium was changed at 3 days in vitro (DIV). After 5 days of culture, the medium was changed to a maintaining medium in which PDGF was replaced by 5 µM cytosine arabinoside to eliminate dividing cells. Half medium changes were performed twice a week.

### Immunocytochemistry

Neuronal cultures at 20 DIV were fixed with 4% paraformaldehyde for 20 min at room temperature, washed three times with PBS, then permeabilized with 0.5% Triton X-100 in PBS containing 10% calf serum, 10% sheep serum, and 0.1% sodium azide. Slides were incubated with anti-MAP-2 monoclonal antibody (Sigma) at a 1:250 dilution and anti-Myt11 affinity-purified polyclonal antibody at a 1:700 dilution overnight at 4°C, then washed three times with PBS. The secondary antibodies, a Cy3-conjugated anti-rabbit Fab and a fluorescein isothiocyanate (FITC)-conjugated anti-mouse IgG (Jackson ImmunoResearch, West Grove, PA), were diluted 1:100 and incubated for 1 hr at room temperature. The slides were washed three times with PBS before incubation with DAPI (4,6-diamido-2-phenylindole; Sigma) at a concentration of 0.01 mg/ml in PBS. Slides were washed in PBS and mounted with Vectashield medium (Vector Labs, Burlingame, CA).

To test the specificity of the antibody, slides were treated with a Myt11 antibody that had been preincubated for 16 hr with a 50-fold excess by weight of antigen, the recombinant His-tagged Myt11 protein described above. The antibody incubations were carried out as detailed above.

Seven-micron-thick sections of paraffin-embedded CNS tissue fixed by perfusion with 4% paraformaldehyde were obtained from Novagen (Madison, WI). Immunostaining with the αMyt1-His polyclonal rabbit antibody (1:50 dilution) or the αMyt11 rabbit polyclonal antibody (1:100 dilution) was performed according to the methods described in Armstrong et al. (1997). Tissue sections from each embryonic (E) day between days E11 and E18 as well as postnatal (P) days 2 and 15 were examined for immunoreactivity with αMyt1-His, while sections from days E15, E17, E18, and P15 were examined for immunoreactivity with αMyt11 antibody. Developing neurons were identified by immunofluorescence with TuJ1 mouse monoclonal antibody (1:400 dilution; BAbCO; Berkeley, CA) which recognizes neuron-specific class IIIβ tubulin that is expressed in neurons coincident with terminal mitosis and accumulates with further differentiation (Lee et al., 1990; Menezes and Luskin, 1994). In double-label immunofluorescence experiments with αMyt11 antibody and TuJ1, cell nuclei were stained for 30 min with DAPI diluted to 0.01 mg/ml in PBS.

Immunoreactivity of cultured cells or tissue sections was detected using a Zeiss Photoscope III either with a 6.3×, 25×, or 63× objective. Images obtained with the 25× objective were photographed with 400ASA TMAX or Ektachrome film and then digitized and imported into Adobe Photoshop. Images obtained with the 63× objective were acquired and restored using the CELLscan image analysis system (Scanalytics Inc.; Billerica, MA) with exhaustive photon reassignment.

### Genbank and Mouse Genome Database

#### Accession Numbers

The Genbank accession number for the mouse Myt1 cDNA is AF004294, and for the mouse Myt11 cDNA is AF004295. The mouse genome database accession number is MGD-JNUM-41157.

## RESULTS

### Sequence Analysis

A partial cDNA clone encoding human *MYT1* was originally isolated by its ability to bind to the human PLP promoter (Kim and Hudson, 1992). Here we report the full-length clone of the mouse counterpart, *Myt1* (Fig. 1). The putative open reading frame is 3,231 nucleotides (1,077 amino acids with a predicted molecular weight of

118 kDa) preceded by 530 nucleotides of 5' untranslated region. The protein contains six zinc finger domains, organized in clusters of two and four zinc fingers, separated by 289 amino acids. The amino acid sequences of the fingers are highly conserved. These features are extremely similar to the human *MYT1* clone, to which the mouse nucleotide sequence shares 89% identity. The amino-terminal part of the protein is highly acidic, containing 46 consecutive residues of glutamic and aspartic acids. There is a relatively large 3' noncoding region and within this region there are 12 copies of the sequence ATTTA. These sequences have been associated with RNA instability and are speculated to mediate selective RNA degradation (Decker and Parker, 1994).

Over 3,400 different messenger RNAs that are expressed in the brain have been identified through expressed sequence tags (EST) (Adams et al., 1993), including an EST-identified clone (EST05024) of 76 amino acids that has over 70% amino acid identity with the four-finger domain of the human *MYT1*. Using the original EST05024 clone as a probe, we isolated a full-length mouse cDNA and named it Myt1-like (*Myt1l*). A rat version of Myt1l has also recently been cloned and named NZF-1 (Jiang et al., 1996). Analysis of the mouse Myt1l nucleotide sequence shows that it contains an open reading frame that could encode 1,182 amino acids with a predicted molecular weight of 130 kDa and a predicted pI of 4.6 (Fig. 2). The protein is organized in clusters of two and three zinc fingers, as well as a single zinc finger near the amino terminus. As with *Myt1*, *Myt1l* contains a highly acidic region near the amino terminus. As seen in Figure 3, these two proteins have a similar organization and share extensive amino acid homologies throughout the protein, especially in the zinc finger domains. The *Xenopus Myt1* fingers (Bellefroid et al., 1996) differ from the respective human gene at only three amino acid positions, and each of these amino acids in the *Xenopus Myt1* is identical with the *Myt1l* sequence. Moreover, the variation between species is minimal, with *Myt1l* from mouse (Fig. 2) and rat (Jiang et al., 1996) displaying 92% amino acid identity and 97% nucleotide identity in the coding region. Secondary structure analysis of both proteins predicts domains with several long  $\alpha$ -helices in the amino-terminal region and the carboxy-terminal region immediately following each zinc finger cluster, implying a possible structural role for these domains.

### Genetic Mapping of *MYT1* and *MYT1L*

The localization of the *MYT1* and *MYT1L* genes to human chromosomes was carried out using a panel of monochromosomal human/rodent cell lines (Fig. 4). On this Southern blot, the *MYT1* probe distinguishes between the mouse (5.5-kb), hamster (4.5-kb), and human (3.8-kb) *MYT1* genomic BamHI fragments. The only

hybrid cell line to display the human *MYT1* band in addition to the rodent fragments (the mouse 5.5-kb band) was the one containing human chromosome 20 (top panel, Fig. 4). The blot containing the panel of human/rodent hybrid cell lines was stripped and subsequently hybridized with the *MYT1L* probe, which distinguishes between the mouse (2.2-kb), hamster (26-kb), and human (22-kb) *MYT1L* genomic BamHI fragments. The hybrid cell line which yielded a human 22-kb band in addition to the mouse 2.2-kb band was the one containing human chromosome 2 (bottom panel, Fig. 4).

### Developmental Time Course of *Myt1* and *Myt1l* mRNA Transcript Levels

The expression of *Myt1* mRNA during rat brain development from embryonic day 11 (E11) to postnatal day 15 (P15) was analyzed on Northern blots (Fig. 5). The mRNA was first detectable at E13 and reached the highest level at E15–E17. Subsequently, the level of *Myt1* mRNA decreased (Fig. 5) and was maintained at very low levels in the adult (Kim and Hudson, 1992).

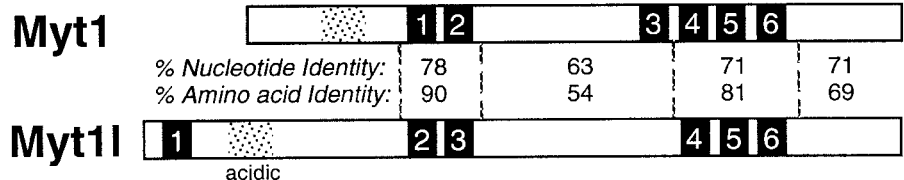
A distinct temporal pattern of gene expression was observed for the other closely related member of the CCHC zinc finger family, *Myt1l*. A major transcript of 7.5 kb was detected at E15, reached a maximum at the day of birth, and subsequently decreased (Fig. 5). *Myt1l* message continued to be expressed at detectable levels in the adult brain. A second *Myt1l* transcript of 2.0 kb was also evident as early as E11, with maximal expression at E15 in rat brain. This transcript may represent an alternatively spliced variant of *Myt1l*. *Myt1l* transcripts of different size (5 kb) were also present in the testis, the only tissue other than brain to display detectable *Myt1* transcripts in a screen including heart, spleen, lung, skeletal muscle, and kidney tissue (data not shown). The tissue-specific expression of *Myt1l* is therefore similar to that previously observed for *Myt1* (Kim and Hudson, 1992), in which the brain was the only tissue with detectable *Myt1* transcripts by Northern analysis.

### Differential Cellular Expression of *Myt1* and *Myt1l* mRNA Transcripts

To determine which cell types of the brain express *Myt1* or *Myt1l* transcripts, Northern analysis was performed using cultures derived from neonatal rat brain and enriched for either astrocytes (As), oligodendrocyte progenitors (Prog), or oligodendrocytes (Oligo). As previously reported, *Myt1* was most abundantly expressed in oligodendrocyte progenitor cells (Fig. 6; Armstrong et al., 1995), and a faint signal was detectable in postnatal day 2 brain (Br) and spinal cord (Sc). Astrocytes had no detectable *Myt1* mRNA, nor did postnatal day 2 rat sciatic nerve (Sn). *Myt1l* transcripts were detected in







### Finger 1

**MYT1 human**                    **KCPTPGCDGTGHVTGLYPHHRSLSGCPHK**  
*Myt1 mouse*                    . . . **A** . . . . .  
*Myt1 xenopus*                    . . . . .  
**MYT1L human(finger 2)** . . . . . **P** . . . . .  
*Myt1l rat (finger 2)*            . . . . .  
*Myt1l mouse (finger 2)*       . . . . .

### Finger 2

**MYT1 human**                    **KCPTPGCTGQGHVNSNRNTHRSLSGCPIA**  
*Myt1 mouse*                    . . . . . **Y** . . . . .  
*Myt1 xenopus*                    . . . . .  
**MYT1L human(finger 3)** . . . . . **H** . . . . . **S** . . . . .  
*Myt1l rat (finger 3)*            . . . . . **R** . . . . . **S** . . . . .  
*Myt1l mouse (finger 3)*       . . . . . **R** . . . . . **S** . . . . .

### Finger 3

**MYT1 human**                    **TCPTPGCDGSGHITGNYASHRSLSGCPLA**  
*Myt1 mouse*                    . . . . .  
*Myt1 xenopus*                    **S** . . . . .  
*Myt1l rat (finger 1)*            **S** . . . . . **VS.K.R.VY** . . . . .  
*Myt1l mouse (finger 1)*       **S** . . . . . **VS.K.R.VY** . . . . .

### Finger 4

**MYT1 human**                    **KCPTPGCDGSGHITGNYASHRSLSGCPRA**  
*Myt1 mouse*                    . . . . .  
*Myt1 xenopus*                    . . . . .  
**MYT1L human(finger 4)** . . . . .  
*Myt1l rat (finger 4)*            . . . . .  
*Myt1l mouse (finger 4)*       . . . . .

### Finger 5

**MYT1 human**                    **KCPVPGCVGLGHIISGKYASHRSASGCPLA**  
*Myt1 mouse*                    . . . . .  
*Myt1 xenopus*                    . . . . . **D** . . . . .  
**MYT1L human(finger 5)** **R** . . . . . **D.Q.T** . . . . .  
*Myt1l rat (finger 5)*            **R** . . . . . **D.Q.T** . . . . .  
*Myt1l mouse (finger 5)*       **R** . . . . . **D.Q.T** . . . . .

### Finger 6

**MYT1 human**                    **TCPTPGCDGSGHTIGSFLTHRSLSGCPRA**  
*Myt1 mouse*                    . . . . . **AN** . . . . .  
*Myt1 xenopus*                    **S** . . . . .  
**MYT1L human(finger 6)** **S** . . . . . **VS** . . . . .  
*Myt1l rat (finger 6)*            **S** . . . . . **VS** . . . . .  
*Myt1l mouse (finger 6)*       **S** . . . . . **VS** . . . . .

**CONSENSUS: CPXPGCXGXGHXXXXXXXXXHRSXXGCP**

Fig. 3. Comparison of the zinc finger regions of *Myt1* and *Myt1l*. The relative positions of zinc fingers in the *Myt1* or *Myt1l* gene are depicted as numbered boxes. The acidic region in both genes is shown by the area filled with dots. The extent of homology between *Myt1* and *Myt1l* is shown for four regions encompassing the six zinc fingers of *Myt1*. Each of the six zinc fingers present in the human amino acid sequence of *MYT1* (Kim and Hudson, 1992) is aligned with the corresponding sequence of either mouse *Myt1* (Fig. 1) or *Xenopus Myt1* (Bellefroid et al., 1996, and direct submission to Genbank:

accession No. U67078), or the human *MYT1L* (this study), rat *Myt1l* (Jiang et al., 1996), or mouse *Myt1l* (Fig. 2). Shading indicates amino acids which were identical for all zinc fingers of this family. The consensus sequence identifies those amino acids which showed no variation between species or between the two gene loci; the other amino acids are indicated by an X. The bold-faced, underlined amino acids within the consensus site represent the cysteines and histidines comprising the zinc coordination domain.



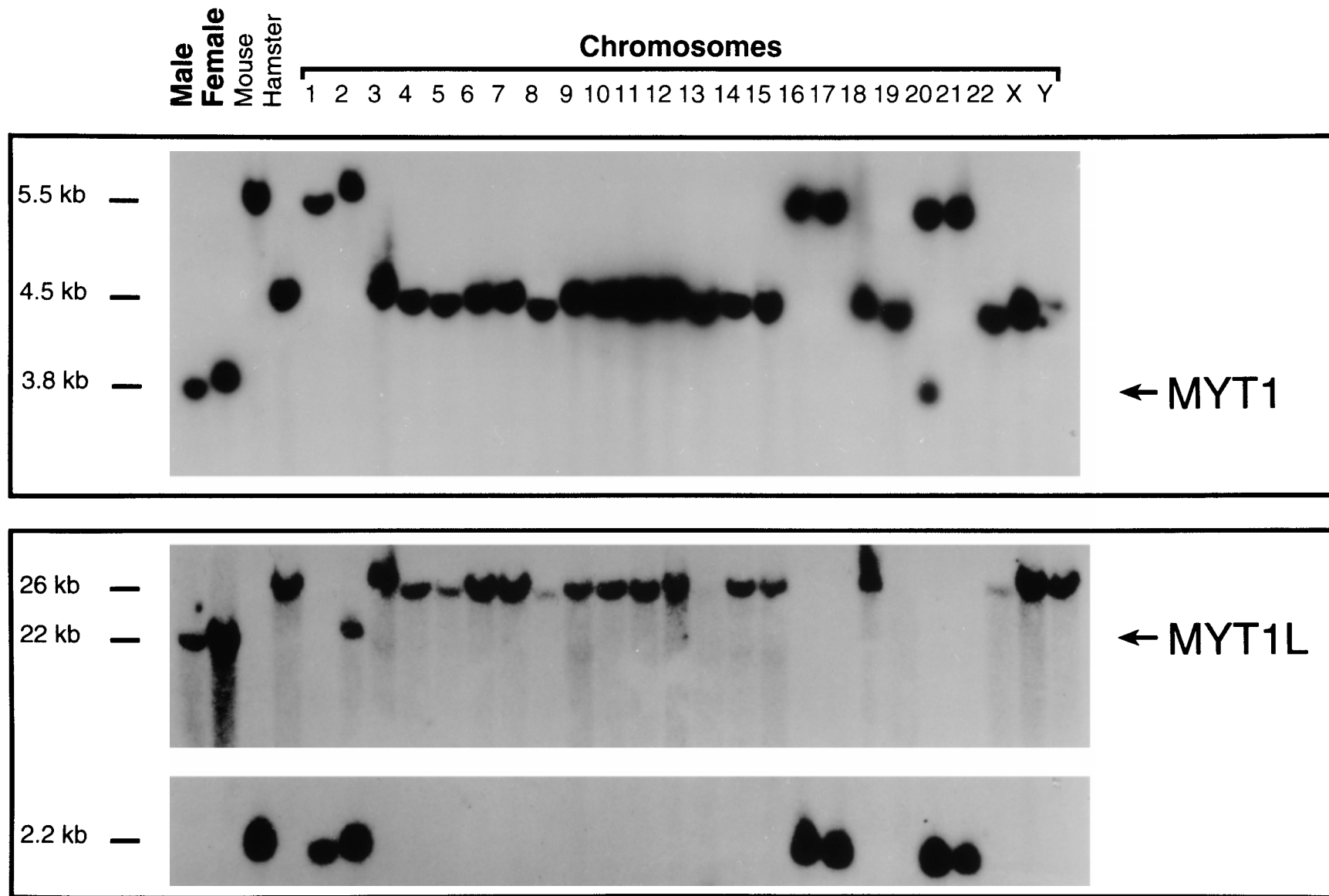


Fig. 4. *MYT1* maps to human chromosome 20 and *MYT1L* maps to human chromosome 2. The Southern blot of BamHI digested genomic DNA features the controls in the first four lanes (labeled male [human], female [human], mouse, and hamster, respectively), followed by the hybrid cell lines, each of which contains a single human chromosome. The sizes of the BamHI fragments are indicated on the left, and an arrow points to the human fragment on the right. The **upper panel** depicts the Southern blot probed with MYT1, and the **lower panel** is the same blot hybridized with the MYT1L probe.

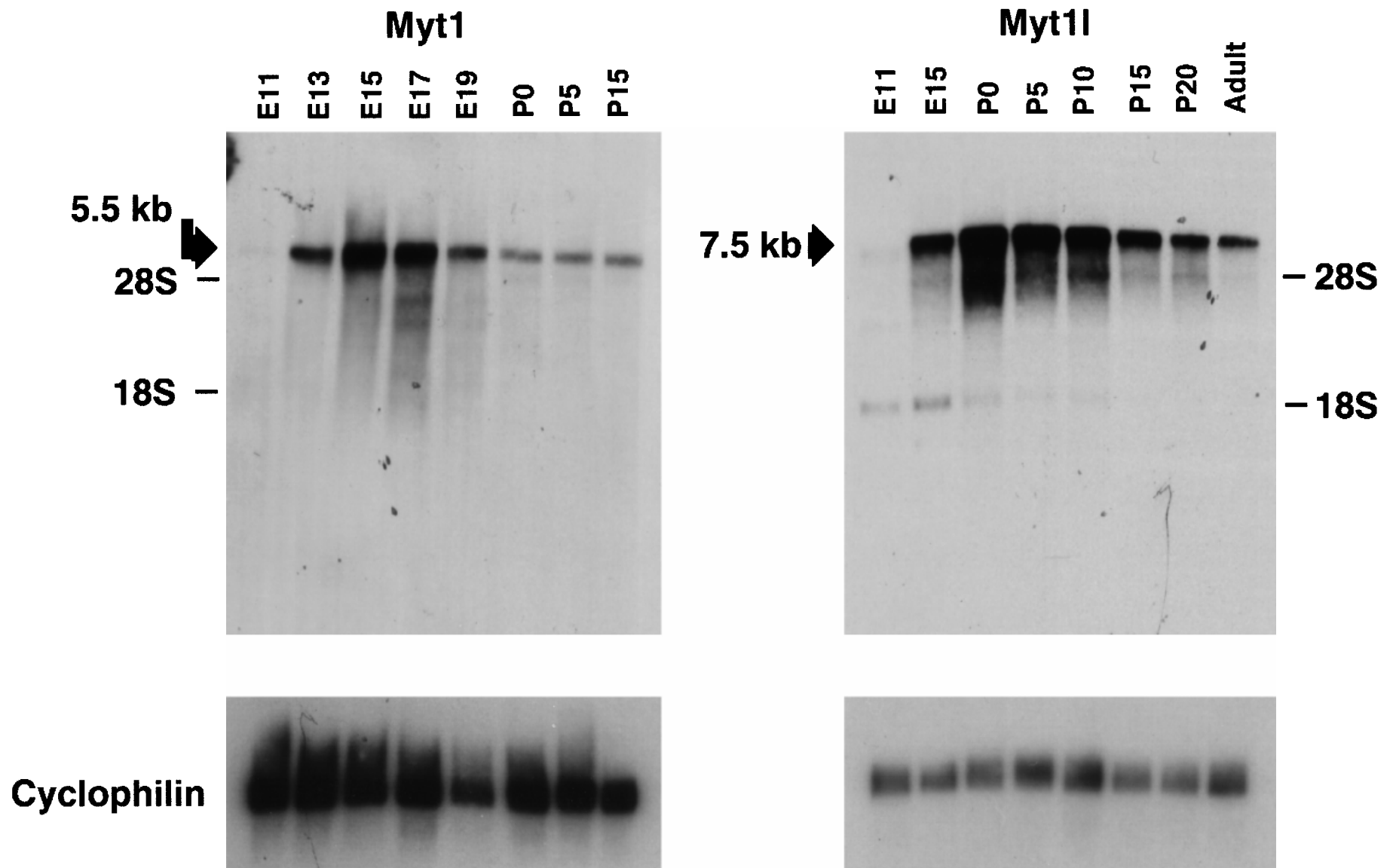


Fig. 5. Northern blot analysis of Myt1 and Myt11 mRNAs during rat brain development. **Top panel:** Poly A+ RNA (1 µg/lane) from different stages of rat brain development were used for the Northern analysis. The blot was hybridized with the riboprobes specific for the rat form of either Myt1 or Myt11. **Bottom panel:** The same blot was stripped and rehybridized with the cyclophilin probe to verify the presence of intact RNA in all lanes.

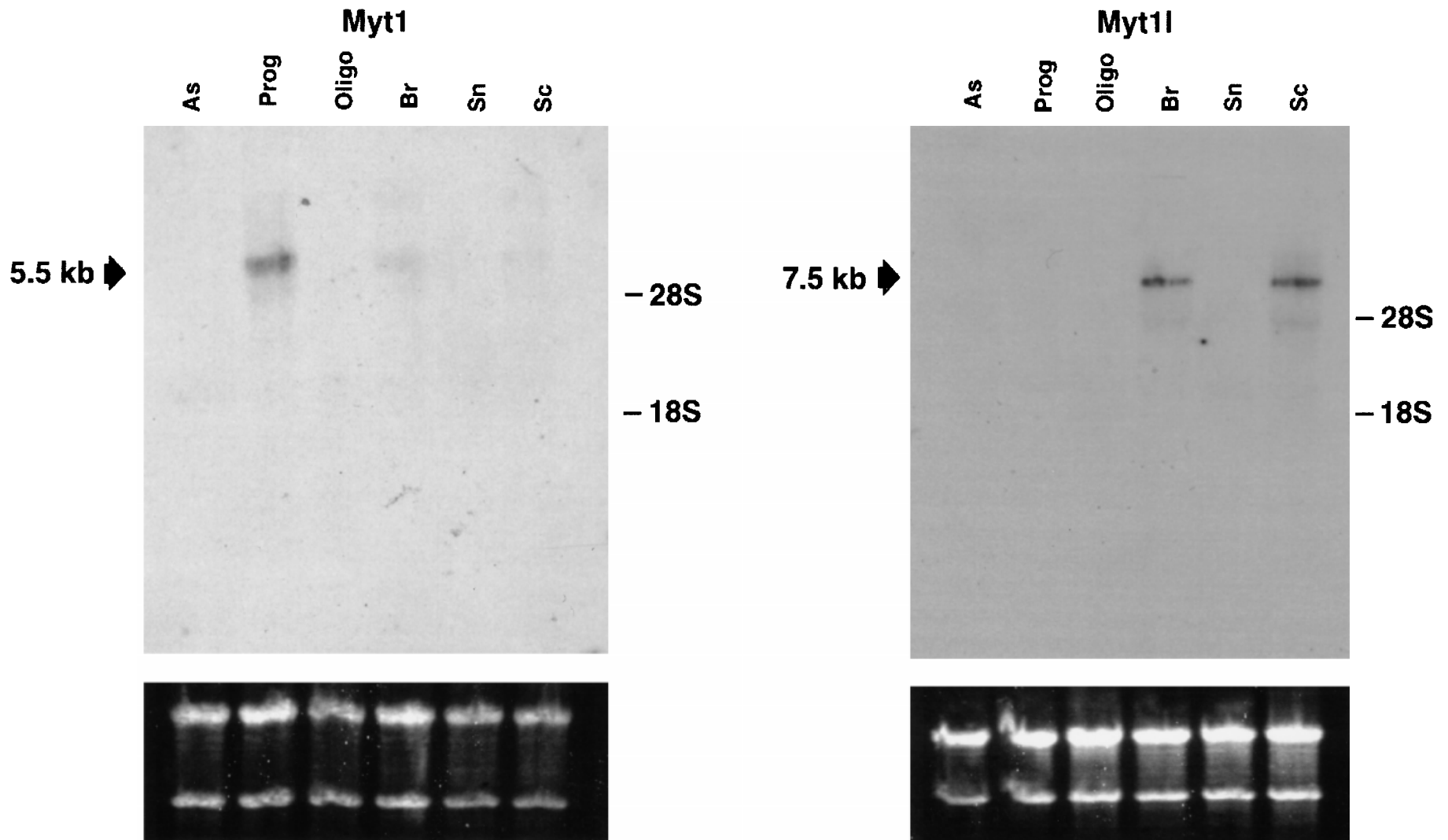


Fig. 6. Northern blot analysis of Myt1 and Myt11 mRNAs in enriched cultures of rat glial cell types. **Top panel:** Total RNA (2  $\mu$ g/lane) obtained from various cell types (As, astrocytes; Prog, progenitors; Oligo, oligodendrocytes) or postnatal day 2 tissues (Br, brain; Sn, sciatic nerve; Sc, spinal cord) were used for the Northern analysis. Positions of the 28S and 18S rRNAs are noted. **Bottom panel:** Ethidium bromide staining of 28S and 18S ribosomal RNA is shown as a control for sample loading.



brain and spinal cord (Fig. 6), but not in cultures enriched for glial cells. The absence of Myt11 expression in astrocytes and oligodendrocytes suggests that Myt11 mRNA in the CNS is restricted to neurons.

This differential expression of Myt1 and Myt11 mRNA transcripts was confirmed by *in situ* hybridization of tissue sections from postnatal day 3 cervical spinal cord. Spinal cord was chosen to readily compare the neuronal and glial cell distribution, as well as functionally diverse neuronal populations. Hybridization with a Myt1-specific probe demonstrated signal in small cells of the ventral white matter and also in motor neurons of gray matter (Fig. 7C). In the dorsal horn, mRNA was also found in the white and gray matter (Fig. 7D), with the strongest signal being associated with small process-bearing cells of the gray matter found in a distribution that did not clearly follow a given sensory neuron lamina but was consistent with a glial cell distribution and morphology.

In contrast to the strong signal in white matter tracts observed with a PLP probe (Fig. 7A,B), hybridization of similar tissue sections with a probe that specifically detects Myt11 mRNA transcripts demonstrated a marked absence of signal in white matter tracts (Fig. 7E,F). But a strong signal for Myt11 was detected in the ventral motor neurons and in cells with the distribution and morphology of sensory neurons found throughout the dorsal horn (Fig. 7E,F). The differential expression of Myt1 versus Myt11 in glial cells was also confirmed by *in situ* hybridization of cultured oligodendrocyte lineage cells (not shown). Consistent with the Northern analysis, cultured neonatal rat oligodendrocyte progenitors exhibited signal for Myt1 which was not detectable in mature oligodendrocytes, and neither progenitors nor oligodendrocytes showed hybridization of the Myt11 probe.

### Differential Cellular Expression of Myt1 and Myt11 Proteins

Using a polypeptide from a region of Myt11 that was not conserved with Myt1, we developed an antibody specific for an amino terminal region of Myt11 (boxed in Fig. 2). As shown in Figure 8, the  $\alpha$ Myt11 antibody did not cross-react with a full-length recombinant Myt1 protein (Fig. 8B, lane 2), although it strongly reacted with a His-tagged Myt11 polypeptide (Fig. 8B, lane 4). Likewise, the  $\alpha$ Myt1-His antibody did not recognize the Myt11 peptide (Fig. 8A, lane 4). However, the  $\alpha$ Myt1-His antibody was raised against the "central domain" of the Myt1 protein (amino acids 541–727), which does not include the highly conserved zinc finger domains but still retains 53% amino acid identity with Myt11 (Fig. 3), presenting the possibility that the  $\alpha$ Myt1-His antibody may cross-react with the central domain of the intact Myt11 protein. In nuclear extracts from E17 rat brain, the

$\alpha$ Myt1-His antibody recognized a band of 165 kD (Fig. 8A, lane 6) as seen previously (Armstrong et al., 1995), while the  $\alpha$ Myt11 antibody recognized a similarly sized band (Fig. 8B, lane 6). Both Myt1 and Myt11 proteins migrate much slower than expected based on their calculated molecular weights (118 and 130 kDa, respectively), suggesting the presence of post-translational modifications. The high molecular weight Myt1 and Myt11 bands were not detectable at postnatal day 6 (Fig. 8A,B, lane 5), consistent with the Northern analysis (Fig. 5) which showed a down-regulation of both transcripts in postnatal brain. Additional lower molecular weight bands were present at both time points and therefore are not likely to represent degradation products of Myt1 or Myt11.

As expected from the *in situ* hybridization analyses, the  $\alpha$ Myt11 antibody immunolabeled the nuclei of large multipolar cells, which were identified in 10 DIV cultures as developing neurons by MAP-2 immunoreactivity (Fig. 9), but did not immunolabel cultured oligodendrocyte lineage cells (data not shown). The  $\alpha$ Myt11 nuclear immunoreactivity was abolished by overnight incubation of the  $\alpha$ Myt11 antibody with the Myt11 peptide antigen (Fig. 9). Interestingly, the nuclear pattern of  $\alpha$ Myt11 immunoreactivity in neurons has a non-homogeneous distribution (Fig. 9) that is very similar to the pattern observed for Myt1 immunoreactivity in oligodendrocyte lineage cells (Armstrong et al., 1995).

### Expression of Myt1 and Myt11 Protein in the Developing CNS

Immunolabeling of tissue sections of embryonic CNS revealed a differential pattern of expression of Myt1 and Myt11 *in vivo*. While the antibody raised against Myt11 is specific for Myt11 (Fig. 8), the affinity-purified antibody to Myt1 ( $\alpha$ Myt1-His; Armstrong et al., 1995) could potentially cross-react with Myt11. Therefore, using the  $\alpha$ Myt1-His antibody we screened sections each day from E11 through E18 for the overall expression of Myt1 (and possibly Myt11), and then at selected timepoints additional sections were immunostained with the  $\alpha$ Myt11 antibody to identify cell populations expressing specifically Myt11.

Within the developing CNS, areas of neuronal differentiation were strongly immunolabeled with  $\alpha$ Myt11 antibody while  $\alpha$ Myt1-His appeared to label both germinal and differentiating areas (Fig. 10). With each antibody, the immunoreactivity was clearly nuclear (Fig. 10), with cytoplasmic immunoreactivity observed much less frequently (data not shown). Neurons were immunolabeled with both antibodies in several distinct CNS regions in which neurons are differentiating, including the developing cerebral cortex as shown in Figure 10. Consistent with the Northern analysis, we did not find

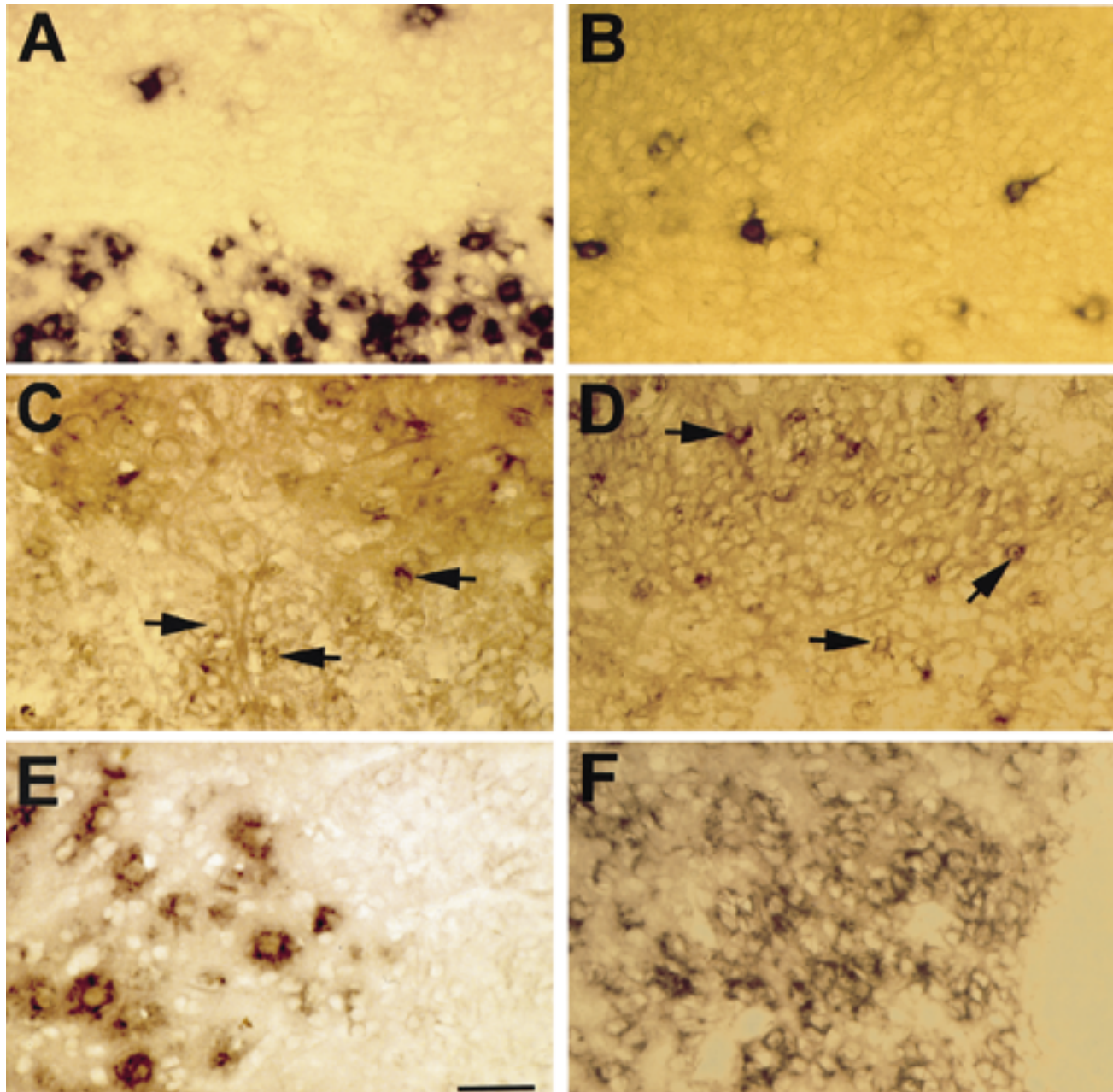


Fig. 7. In situ hybridization for PLP, Myt1, and Myt11. Hybridization of each digoxigenin-labeled riboprobe to tissue sections, from postnatal day 3 rat cervical spinal cord, detected by anti-digoxigenin antibody conjugated with alkaline phosphatase and reacted with NBT-BCIP substrate. Ventral areas are shown on the left (**A,C,E**) and dorsal areas are shown on the right (**B,D,F**). **A** and **B** show detection of PLP mRNA transcripts in oligodendrocytes concentrated in the ventral white matter (**A**) and distributed within the ventral gray matter (**A**) and dorsal gray matter (**B**). **C** and **D** show detection with the Myt1 probe which demonstrates signal in small cells of the ventral white matter (examples indicated by arrows in the lower

half of **C**) and in much larger cells in the ventral horn gray matter (upper half of **C**). Signal from hybridization with the Myt1 probe is also evident within cells scattered throughout the dorsal horn gray matter (examples indicated by arrows in **D**). **E** and **F** show detection with the Myt11 probe which demonstrates signal in the large cells within the ventral gray matter (**E**, left side of field) but not within cells of the ventrolateral white matter (**E**, right side of field). Signal from hybridization with the Myt11 probe is also evident within densely packed cells of the dorsal horn gray matter (**F**) but is again absent from the white matter (**F**, dorsal column along right edge of field). Scale bar = 50  $\mu$ m.

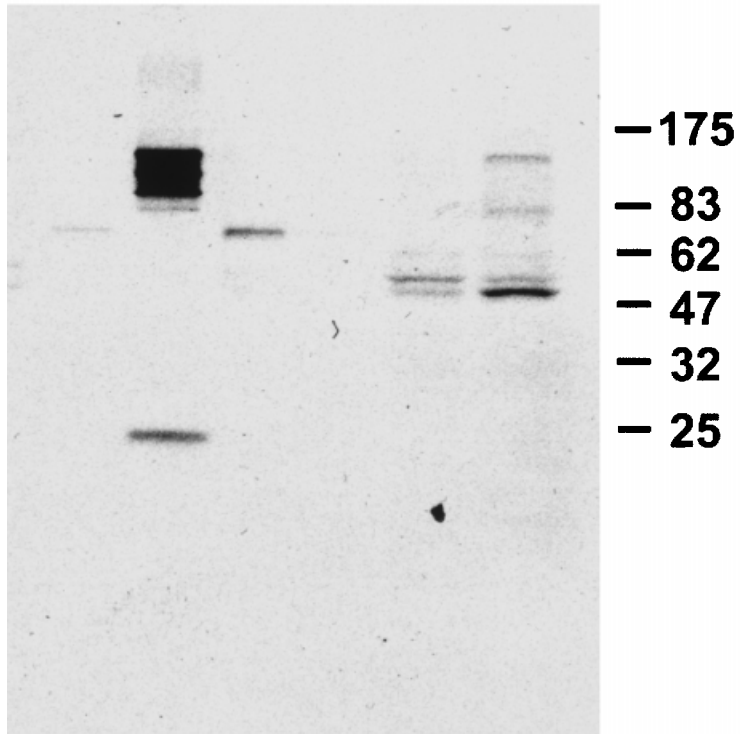
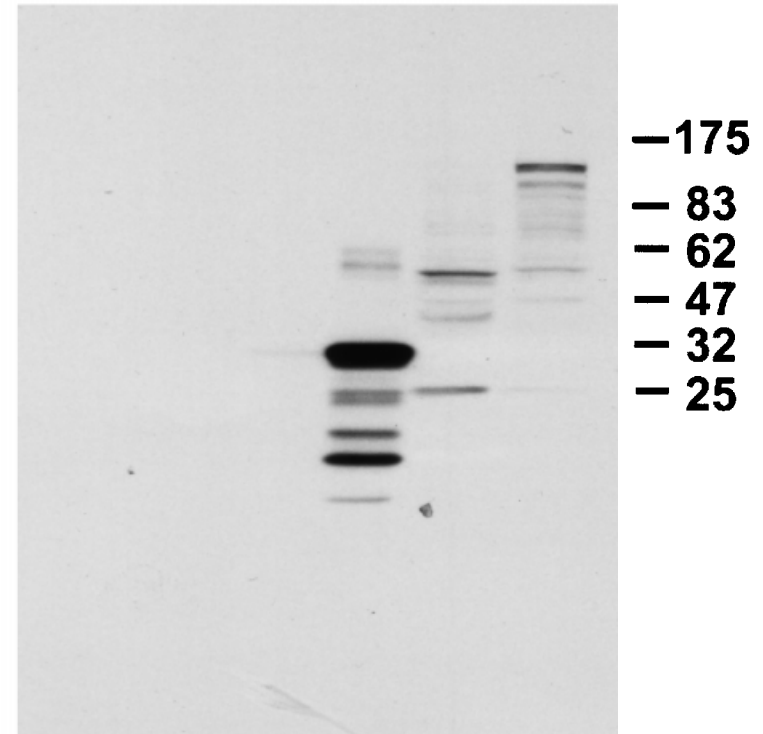
**A****1 2 3 4 5 6****B****1 2 3 4 5 6**

Fig. 8. Immunoblot analysis using anti-Myt1 and anti-Myt11 antibodies. Duplicate blots were incubated with either anti-Myt1 (A) or anti-Myt11 antibody (B). Lanes 1 and 3 contain the control extracts prepared from *Escherichia coli* without induction. Lanes 2 and 4 contain the *E. coli*-expressed extracts of Myt1 (A, lane 2, 165 kd), and Myt11 (B, lane 4, 30 kd). The respective control extracts from uninduced *E. coli* are shown in lanes 1 (Myt1) and 3 (Myt11). The anti-Myt1 antibody does not cross-react with any bands in *E. coli* expressed Myt11 (A, lane 4), nor does the anti-Myt11 antibody cross-react with any bands in the Myt1 lane (B, lane 2). Lanes 5 and 6 contain the rat brain nuclear extracts at ages postnatal day 6 and embryonic day 17, respectively. Molecular sizes (in kilodaltons) are noted at the right.



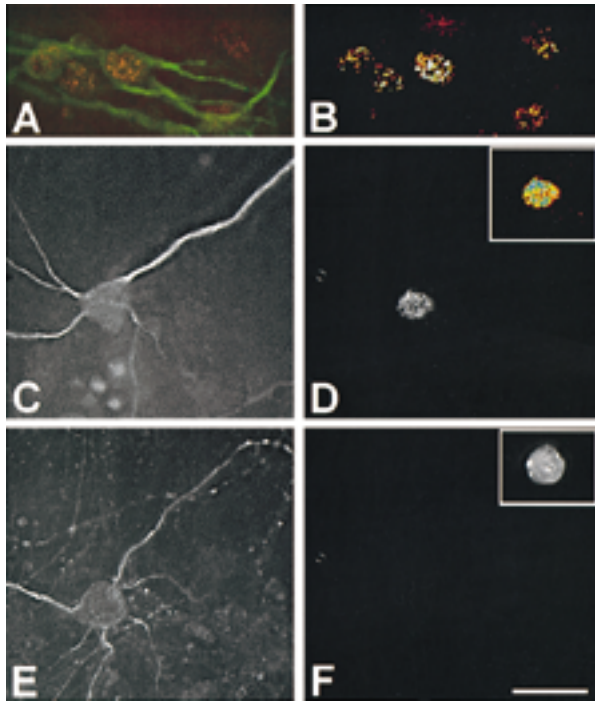


Fig. 9. Immunolabeling of cultured neurons with  $\alpha$ Myt11 antibody. Neurons from E16 rat forebrain grown in culture for 10 days were fixed, double immunolabeled with anti-MAP-2, detected with a fluorescein-conjugated anti-mouse IgG (A in green, C,E), and with  $\alpha$ Myt11, detected with a Cy3-conjugated anti-rabbit IgG (A in red, B,D,F). A,B: The  $\alpha$ Myt11 immunoreactivity (A, red) appears as a punctate pattern within the nucleus of a neuron, identified by anti-MAP-2 immunoreactivity (A, green) in the cytoplasm of the cell body and processes. In B, the  $\alpha$ Myt11 nuclear pattern of the same cell is more clearly distinguished by pseudocoloring that renders the gradient of immunostaining intensity as a range of colors with the highest intensity pixels appearing white. Several adjacent cells are also in this field but are only partially represented in this 0.25- $\mu$ m optical section. C,D: A neuron with characteristic multipolar processes is immunolabeled with MAP-2 (C) and shows nuclear immunoreactivity for  $\alpha$ Myt11 (D, and pseudocolored in inset). E,F: A MAP-2 immunolabeled neuron (E) similar to that shown above does not show nuclear  $\alpha$ Myt11 immunoreactivity after overnight incubation of  $\alpha$ Myt11 antibody with the Myt11 antigen. The inset in F shows the same cell with DAPI nuclear staining to show the nuclear integrity. All images are 0.25- $\mu$ m optical sections obtained with a 63 $\times$  objective using the CELLscan image analysis system with exhaustive photon reassignment. Scale bar = 25  $\mu$ m for A–F.

$\alpha$ Myt11-His immunoreactivity in the CNS at E11 but observed weak signal beginning at E12 and increasing thereafter. Between E15 and E18 the distribution of differentiating neurons becomes much more widespread (see Altman and Bayer, 1995), and the immunolabeling with both antibodies became similarly more widely

distributed over this period. Neuroepithelial and secondary germinal matrix areas, including the subventricular zone, generally contained a majority of cells labeled with  $\alpha$ Myt11-His but were not as well labeled throughout with the  $\alpha$ Myt11 antibody (Fig. 10). Immunolabeling of the subventricular zone with  $\alpha$ Myt11-His continues postnatally and into adulthood (Armstrong et al., 1995, 1997). In comparison, by E15 immunolabeling of neurons with an antibody to TuJ1, which recognizes neurons either during or immediately following terminal mitosis and accumulates with further differentiation (Lee et al., 1990; Menezes and Luskin, 1994), was widespread throughout the CNS except for proliferative zones. Double immunolabeling of cells in areas of neuronal differentiation with TuJ1 and  $\alpha$ Myt11 antibodies demonstrated that not all TuJ1-immunolabeled cells are immunolabeled with  $\alpha$ Myt11 (Fig. 10). Since TuJ1 immunolabels all postmitotic neurons, these results suggest that either Myt11 is expressed in only a subset of differentiating neurons or that Myt11 is expressed in differentiating neurons shortly after expression of TuJ1 commences. This may also be the case with peripheral neurons based upon our preliminary results of  $\alpha$ Myt11 immunostaining of dorsal root ganglia neurons (data not shown). By P15, Myt11 protein expression is evident in limited sets of neuronal subtypes, including within the hippocampal formation. Further studies of the postnatal expression of MYT11 are required to correlate the point at which MYT11 expression is down-regulated relative to the development of specific neuronal cell types throughout the CNS.

## DISCUSSION

In the present study, we describe the chromosomal localization and further characterize the expression of Myt1, the prototypic member of a novel CCHC class of zinc finger proteins. We also present the cloning, chromosomal localization, and characterization of a closely related member of this class, Myt11. The development and application of specific probes that distinguish Myt1 and Myt11 (based on the unique 3' untranslated region of each transcript), together with the preparation of an antibody specific for Myt11, has allowed identification of the specific cell types expressing each zinc finger gene. Preliminary *in situ* hybridization studies (Dent et al., 1993), using a probe that did not distinguish between Myt1 and Myt11, revealed transcripts in diverse neuronal populations throughout the developing CNS. Our present Northern blot analyses (Fig. 5) show that both Myt1 and Myt11 are expressed in developing brain beginning around E13–E15, with a peak transcript level for Myt1 appearing at E15–17 while the peak for Myt11 appeared close to birth. Our *in situ* hybridization and immunostain-

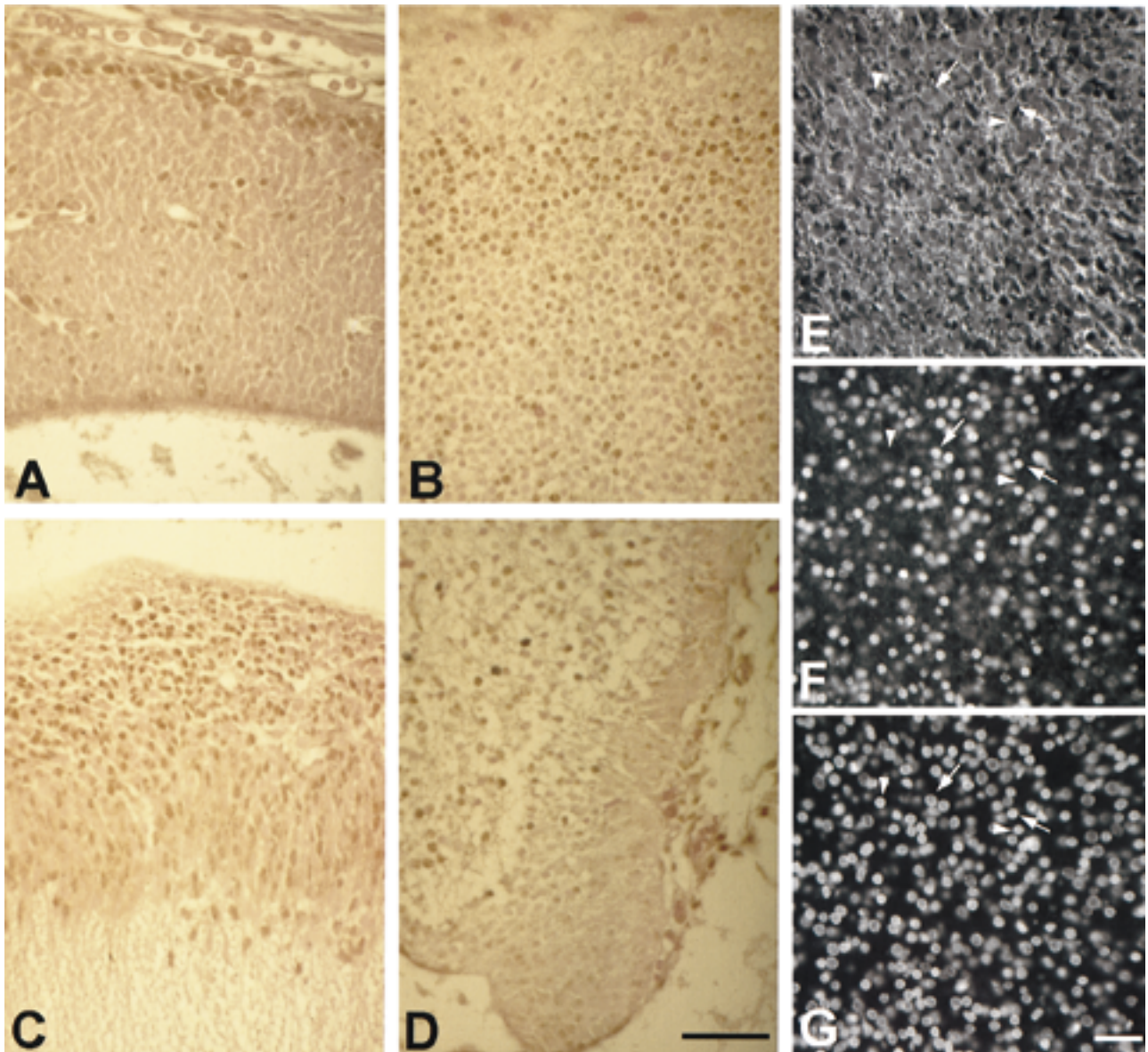


Fig. 10. Immunostaining of embryonic CNS for Myt1 and Myt11. Sagittal sections of developing rat embryos immunostained with  $\alpha$ Myt1-His (A,C), with  $\alpha$ Myt11 (B,D), or multi-labeled with TuJ1 (E),  $\alpha$ Myt11 (F), and DAPI (G). Examples of immunostaining of developing cortex at E15 (A) or E18 (B) show an expanding superficial neuronal differentiation area with nuclear immunoreactivity (brown DAB reaction product against pink eosin counterstain) for  $\alpha$ Myt1-His (A) and  $\alpha$ Myt11 (B). An example of immunostaining of CNS neuroepithelium (C, E14 tegmentum) shows nuclear immunoreactivity with  $\alpha$ Myt1-His in the densely packed neuroepithelial cells (C) that is not observed with  $\alpha$ Myt11 (not shown). An example of immunostaining of a CNS secondary germinal matrix area (D, E18 cerebellum) shows nuclear immunoreactivity with  $\alpha$ Myt11 that is present in dispersed cells in the area of neuronal differentiation but is not marked in the proliferative area

(densely packed cells toward the right, caudal border of the tissue). Nuclei of cells in both the secondary germinal matrix area and the differentiation area of the E18 cerebellum are immunolabeled with  $\alpha$ Myt1-His (not shown). E–G show multi-label immunofluorescence of the E18 cerebellar neuronal differentiation area to demonstrate developing neurons, immunolabeled with TuJ1 (E, detected with fluorescein), that range from positive (arrows) to negative (arrowheads) for  $\alpha$ Myt11 immunoreactivity (F, detected with Cy3) associated with the nuclei (G, detected with DAPI). The nuclear  $\alpha$ Myt11 immunoreactivity exhibits a range of intensities and appears as punctate in some less intensely labeled cells but more completely fills the nucleus in very intensely labeled cells because of overexposure to convey the less intense signal. All images are photographs of 7- $\mu$ m-thick sections taken with a 25 $\times$  objective. Scale bars = 50  $\mu$ m.



ing results (Figs. 7, 10) now demonstrate the specific neural cell populations expressing Myt1 and Myt11.

Our present results of Myt1 expression extend previous studies indicating that Myt1 is expressed in neural precursor cells. We observed Myt1 immunoreactivity in neuroepithelial germinal zones of the CNS in tissues from embryonic (Fig. 10), early postnatal (Armstrong et al., 1995), and adult (Armstrong et al., 1997) ages. The onset and peak of Myt1 mRNA transcript levels correlate well with the rapid increase of oligodendrocyte progenitors around E16–E18 (LeVine and Goldman, 1988; Goynes et al., 1994). Based upon previous studies (Gogate et al., 1994; Armstrong et al., 1995), the Myt1 signal in white matter reflects expression of Myt1 in oligodendrocyte progenitors. This interpretation is also supported by the comparison with the expression of PLP mRNA in oligodendrocytes within the same regions of tissue (Fig. 7). Interestingly, Myt1 appears to be expressed in precursors of both neuronal and glial lineages and to be down-regulated in association with terminal differentiation (Armstrong et al., 1995; Bellefroid et al., 1996). However, the down-regulation of Myt1 may vary between cell types or environmental influences, since rat spinal cord motoneurons continued to have detectable Myt1 signal at postnatal day 3 (Fig. 7). In the adult, neurons do not express detectable levels of Myt1 (Armstrong et al., 1997).

In contrast to Myt1, Myt11 was not found in glial cells. Myt11 transcripts were not detected in glial populations by either our *in vitro* or *in vivo* analyses using Northern blot and *in situ* hybridization techniques (Figs. 6, 7). Nor was Myt11 protein found in glial cells by immunocytochemical methods (Fig. 10). Myt11 mRNA transcripts were most abundant in prenatal brain when the majority of neurons are developing. Myt11 protein appears to be expressed in neurons after terminal mitosis, based upon double immunofluorescence with  $\alpha$ Myt1 and TuJ1 antibodies and based upon the overall lack of Myt11 in neural proliferative zones (Fig. 10). Our findings are supported by the demonstration that transcripts encoding Myt11 (also referred to as png-1) are present in differentiating neurons but not in bromodeoxyuridine-labeled proliferative neuroblasts (Weiner and Chun, 1997). Thus, the temporal and neuroanatomical distribution of Myt11 expression suggests an important role for Myt11 in neuronal differentiation.

The Myt1 family has been highly conserved during evolution, with respect to variation both between species and between family members. For example, the zinc finger domains of *Xenopus* and human Myt1 are strikingly similar, sharing 98% amino acid identity. The two family members (Myt1 and Myt11) likewise display a high degree of identity (91% for the finger regions). Inspection of the 35 zinc fingers that have been sequenced

in the Myt1 family (Fig. 3) reveals the following strictly preserved consensus, where the underlined residues represent the tetrahedral coordination sites of zinc binding to cysteine and histidine residues: CPXPGCXGXGHX<sub>7</sub>HRSX<sub>2</sub>GCP. The additional invariant histidine residue is of note, since it is conceivable that this residue also participates in metal coordination, in a Cys-X<sub>4</sub>-Cys-X<sub>4</sub>-His-X<sub>7</sub>-His-X<sub>5</sub>-Cys arrangement. The large number of invariant proline and glycine residues in this consensus is also of interest, as the lack of secondary structure typical of zinc fingers is probably attributable to the interference by these two amino acids with  $\alpha$ -helical formation.

Myt1 is a nuclear DNA-binding protein that recognizes a site in the promoter of the myelin PLP gene (Kim and Hudson, 1992). The repertoire of binding sites to which Myt1 displays high affinity is a broad one, rich in G residues (Hudson et al., 1995). The *Xenopus* form of Myt1 was found to bind with highest affinity to the consensus site AAAGTTT (Bellefroid et al., 1996), which was surprising in view of the near identity of the vertebrate and invertebrate zinc finger domains of Myt1. This discrepancy probably arises from carrying out excessive cycles of a random site selection assay to determine the target site of binding, as the final binding sites isolated by these assays are high affinity but may not reflect the *in vivo* binding sites. This appears to be the case for the *Xenopus* Myt1, as the binding site identified corresponds to a spacer element in the repetitive 5S ribosomal RNA-encoding transcription units (Bellefroid et al., 1996), yet Myt1 immunoreactivity is clearly excluded from nucleoli in vertebrate cells (Armstrong, unpublished observations). The recognition sites for Myt1 and Myt11 are likely to be similar, given the extreme conservation between the zinc finger domains of the two proteins (Fig. 3) and the ability of the Myt11 protein to bind to an oligonucleotide containing the PLP site that was originally employed to clone Myt1 (Kim and Hudson, 1992; Jiang et al., 1996). How the Myt1 family members function in the control of gene expression is still unknown. It is unlikely that this family behaves as classic transcriptional activators. In transient transfection assays, Myt1 has a minor effect on transcription from the PLP promoter (J. Berndt, J.G.K., and L.D.H., unpublished results); similarly, Myt11 has minimal impact on the transcriptional activity of reporter plasmids containing Myt11-binding sites (Jiang et al., 1996). The intriguing localization of Myt1 in discrete subnuclear domains (Armstrong et al., 1995) together with the structure of the Myt1 proteins, in which multiple DNA-binding domains are organized into widely separated clusters, is consistent with the possibility that this family of proteins may perform an architectural role in assembling transcriptionally active complexes in the nucleus.



The mapping of *MYT1* and *MYT1L* to human chromosome 20 and 2, respectively, was further refined by linkage analysis in the mouse. The *Myt1* gene was located on mouse chromosome 2, with the gene order and recombination fractions for each pair of loci in a (NFS/N × *M. spretus*) × *M. spretus* or C58/J backcross expressed as follows: centromere (Hc2)-*Src*-(8/89)-*Cd40*-(8/95)-*Pck1*-(3/95)-*Myt1*-(4/100)-*Oprl*. (M.S. Lyu, J.G.K., L.D.H., and C.A. Kozak, Mouse genome database accession #MGD-JNUM-41157). This localization confirms that reported for NZF-2 (Jiang et al., 1996), demonstrating that NZF-2 is indeed the mouse form of Myt1. The mouse gene is in a region of conserved synteny with the human chromosome 20 (Siracusa et al., 1996), where the human *MYT1* gene was mapped in this study (Fig. 4). The *Myt1l* gene was localized to mouse chromosome 12, with the gene order and recombination frequencies for each pair of loci in *M.m. musculus* crosses and *M. spretus* crosses expressed as genetic distance in centimorgan ± the standard error: centromere (*Hc12*)-*Plcd2*-(11.5 ± 4)-*Myt1l*-(0.8 ± 0.7)-*Dld*-(0.6 ± 0.6)-*Twist*, *Lamb1-1*-(1.9 ± 1.1)-*Ahr* (M.S. Lyu, J.G.K., L.D.H., and C.A. Kozak, Mouse Genome Data base). This localization is consistent with that reported for NZF-1 (Jiang et al., 1996), indicating that the rat NZF-1 and the mouse Myt1l (this study) represent the same gene. The human *MYT1L* gene was located on human chromosome 2 (Fig. 4), which contains regions of conserved synteny with mouse chromosome 12 (D'Eustachio and Riblet, 1996). The mapping of *MYT1L* to the 2p24 region of human chromosome 2 should facilitate the identification of diseases involving neuronal development. Likewise, the predicted map location of *MYT1* on human 20q13 adds to the arsenal of genes that can be employed to screen patients with white matter disorders, such as Pelizaeus Merzbacher disease (PMD) patients (reviewed in Hodes et al., 1993), whose disease is not inherited in an X-linked manner. Patients with *MYT1* mutations may be anticipated to have additional symptoms beyond those observed in the classical cases of PMD disease, as the *Myt1* gene is expressed very early in development. Also, the expression of *Myt1* in the nervous system is broader than that observed for PLP, as neuronal populations express *Myt1* for a restricted period in their development (Fig. 7).

Our characterization of *Myt1l*, another member of the *Myt1* family, has refined the features of this emerging class of zinc finger transcription factors in the nervous system. The partially overlapping expression of the two members, one primarily in neural precursors including oligodendrocyte progenitors, where at least one target site of action is the myelin PLP gene, and the other in differentiating neurons, suggests that both members of this family have roles in the development of the central nervous system. The persistence of *Myt1* expression in

adult rodent and human CNS in neural precursors of the subventricular zone (Armstrong et al., 1997) and in oligodendrocyte progenitors within the white matter (Gogate et al., 1994) suggests a potential role for *Myt1* in CNS regenerative responses. This hypothesis is further supported by preliminary results that indicate a reappearance of *Myt1* in response to demyelination in rodent (Hudson et al., 1997) and human CNS (R. Armstrong, C. Lucchinetti, J. Kim, M. Rodriguez, and L. Hudson, unpublished observations). Thus, further delineating the role of these zinc finger proteins may reveal mechanisms of neural development that are called into play during CNS regenerative responses.

## ACKNOWLEDGMENTS

The authors thank Drs. M.S. Lyu and Christine A. Kozak for carrying out the mapping studies of *Myt1* and *Myt1l* in the mouse. The authors gratefully acknowledge the input of Drs. Myrna Dent and Rhona Mirsky in the initial in situ hybridization studies and also thank Dr. Boris Zalc for sharing his in situ hybridization results. We also thank Dr. Anne Schaffner for help in preparation of embryonic rat tissues. Dr. Karen Chandross provided helpful critique of the manuscript. This work was supported in part by funds from the intramural program of NINDS to L.D.H., by a National Multiple Sclerosis fellowship to J.G.K., by a Deutsche Forschungsgemeinschaft fellowship to C.W., and by USUHS grant R070CB to R.C.A. A.R. was a Howard Hughes Medical Institute scholar.

## REFERENCES

- Adams MD, Kerlavage AR, Fields C, Venter JC (1993): 3,400 new expressed sequence tags identify diversity of transcripts in human brain. *Nature* 4:256–267.
- Agoston DV, Eiden LE, Brenneman DE (1991): Calcium-dependent regulation of the enkephalin phenotype by neuronal activity during early ontogeny. *J Neurosci Res* 28:140–148.
- Altman J, Bayer SA (1995): "Atlas of Prenatal Rat Brain Development." Boca Raton, FL: CRC Press.
- Armstrong RC, Kim JG, Hudson LD (1995): Expression of myelin transcription factor I (MyTI), a "zinc-finger" DNA-binding protein, in developing oligodendrocytes. *Glia* 14:303–321.
- Armstrong RC, Migneault A, Shegog ML, Kim JG, Hudson LD, Hessler RB (1997): High grade human brain tumors exhibit increased expression of myelin transcription factor I (MYT1), a zinc finger DNA-binding protein. *J Neuropathol Exp Neurol* 56:in press.
- Berg JM, Shi Y (1996): The galvanization of biology: a growing appreciation for the roles of zinc. *Science* 271:1081–1085.
- Bellefroid EJ, Bourguignon C, Hollemann T, Ma Q, Anderson DJ, Kintner C, Pieler T (1996): X-MyT1, a Xenopus C2HC-type zinc finger protein with a regulatory function in neuronal differentiation. *Cell* 87:1191–1202.

- Berndt J, Kim J, Hudson LD (1992): Cis regulatory elements required for expression of the myelin proteolipid protein gene. *J Biol Chem* 267:14730–14737.
- Chomczynski P, Sacchi N (1987): Single-step method of RNA isolation by acid guanidinium thiocyanate-phenol-chloroform extraction. *Anal Biochem* 162:156–159.
- Cleveland DW, Lopata MS, MacDonald RJ, Cowan NJ, Rutter WJ, Kirschner MS (1980): Number and evolutionary conservation of  $\alpha$ - and  $\beta$ -tubulin and cytoplasmic  $\beta$  and  $\gamma$ -actin genes using specific cloned cDNA probes. *Cell* 20:95–105.
- Covey SN (1986): Amino acid sequence homology in gag region of reverse transcribing elements and the coat protein gene of cauliflower mosaic virus. *Nucleic Acids Res* 14:623–633.
- Decker CJ, Parker R (1994): Mechanisms of mRNA degradation in eukaryotes. *Trends Biochem Sci* 19:336–340.
- Dent MAR, Mirsky R, Jessen KR, Hudson L (1993): Expression of the myelin transcription factor 1 in developing rat nervous system. *Soc Neurosci Abstr* 19:1725.
- D'Eustachio P, Riblet R (1996): Mouse chromosome 12. *Mamm. Genome [Suppl]* 6:S221–231.
- Gogate N, Verma L, Zhou JM, Milward E, Rusten R, O'Connor M, Kufta C, Kim J, Hudson L, Dubois-Dalcq M (1994): Plasticity in the adult human oligodendrocyte lineage. *J Neurosci* 14:4571–4587.
- Goyne GE, Warrington AE, DeVito JP, Pfeiffer SE (1994): Oligodendrocyte precursor quantitation and localization in perinatal brain using a retrospective bioassay. *J Neurosci* 14:5365–5372.
- Gu J, Stephanson CG, Iadarola MJ (1994): Recombinant proteins attained to a nickel-NTA column: use in affinity purification. *Biotechniques* 17:257–262.
- Hodes ME, Pratt VM, Dlouhy SR (1993): Genetics of Pelizaeus-Merzbacher disease. *Dev Neurosci* 15:383–394.
- Hudson LD, Ko N, Kim JG (1995): Control of myelin gene expression. In Richardson WD, Jessen KR (eds): "Glial Cell Development: Basic Principles and Clinical Relevance." London: Bios Scientific Pub, pp 101–121.
- Hudson LD, Kim JG, Wiese C, Yao D-L, Liu X, Webster H deF, Agoston vD, Armstrong R (1997): Transcriptional controls in the oligodendrocyte lineage. In Jeserich G, Althaus HH, Richter-Landsberg C, Heumann R (eds): "Molecular Signaling and Regulation in Glial Cells: A Key to Remyelination and Functional Repair." Berlin: Springer-Verlag, pp 182–190.
- Jiang Y, Yu VC, Buchholz F, O'Connell S, Rhodes SJ, Candeloro C, Xia Y-R, Luis AJ, Rosenfeld MG (1996): A novel family of cys-cys, his-cys zinc finger transcription factors expressed in developing nervous system and pituitary gland. *J Biol Chem* 271:10723–10730.
- Kim JG, Hudson LD (1992): Novel member of the zinc finger superfamily: A C2-HC finger that recognize a glia-specific gene. *Mol Cell Biol* 12:5632–5639.
- Lee MK, Tuttle JB, Rebhun LI, Cleveland DW, Frankfurter A (1990): The expression and posttranslational modification of a neuron-specific  $\beta$ -tubulin isotype during chick embryogenesis. *Cell Motil Cytoskeleton* 17:118–132.
- LeVine SM, Goldman JE (1988): Embryonic divergence of oligodendrocyte and astrocyte lineages in developing rat cerebrum. *J Neurosci* 8:3992–4006.
- Milner RR, Sutcliffe JG (1983): Gene expression in rat brain. *Nucleic Acids Res* 11:5497–5520.
- Menezes JRL, Luskin MB (1994): Expression of a neuron-specific tubulin defines a novel population in the proliferative layers of the developing telencephalon. *J Neurosci* 14:5399–5416.
- Siracusa LD, Morgan JL, Fisher JK, Abbott CM, Peters J (1996): Mouse chromosome 2. *Mamm. Genome [Suppl]* 6:S51–S63.
- Wiese C, Kim JG, Warrington A, Hudson LD (1995): Novel zinc finger proteins expressed in the nervous system. *Soc Neurosci Abstr* 21:425.14.